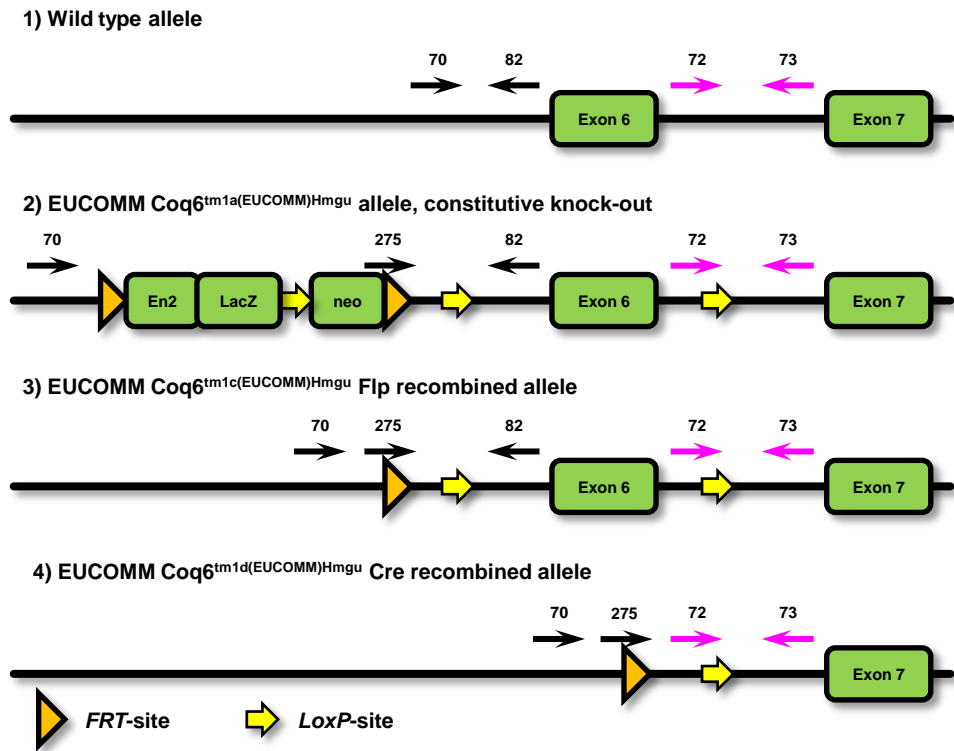
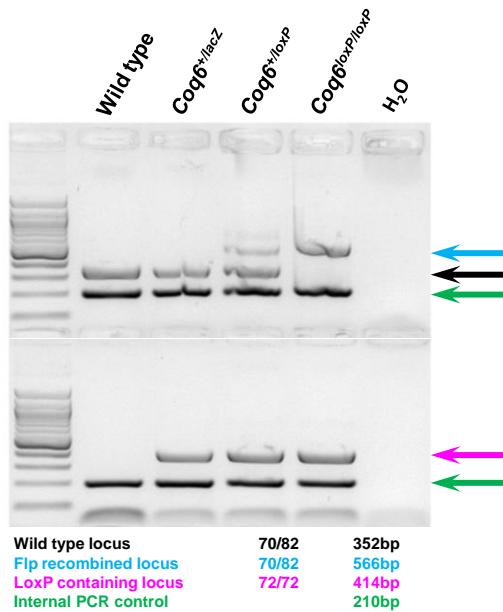
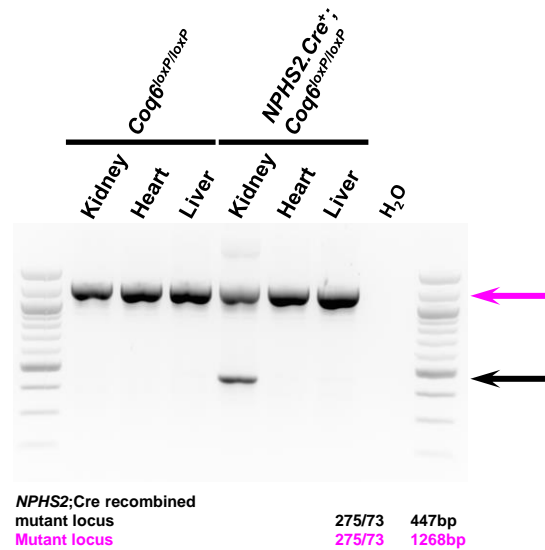


SUPPLEMENTARY DATA TABLE OF CONTENTS

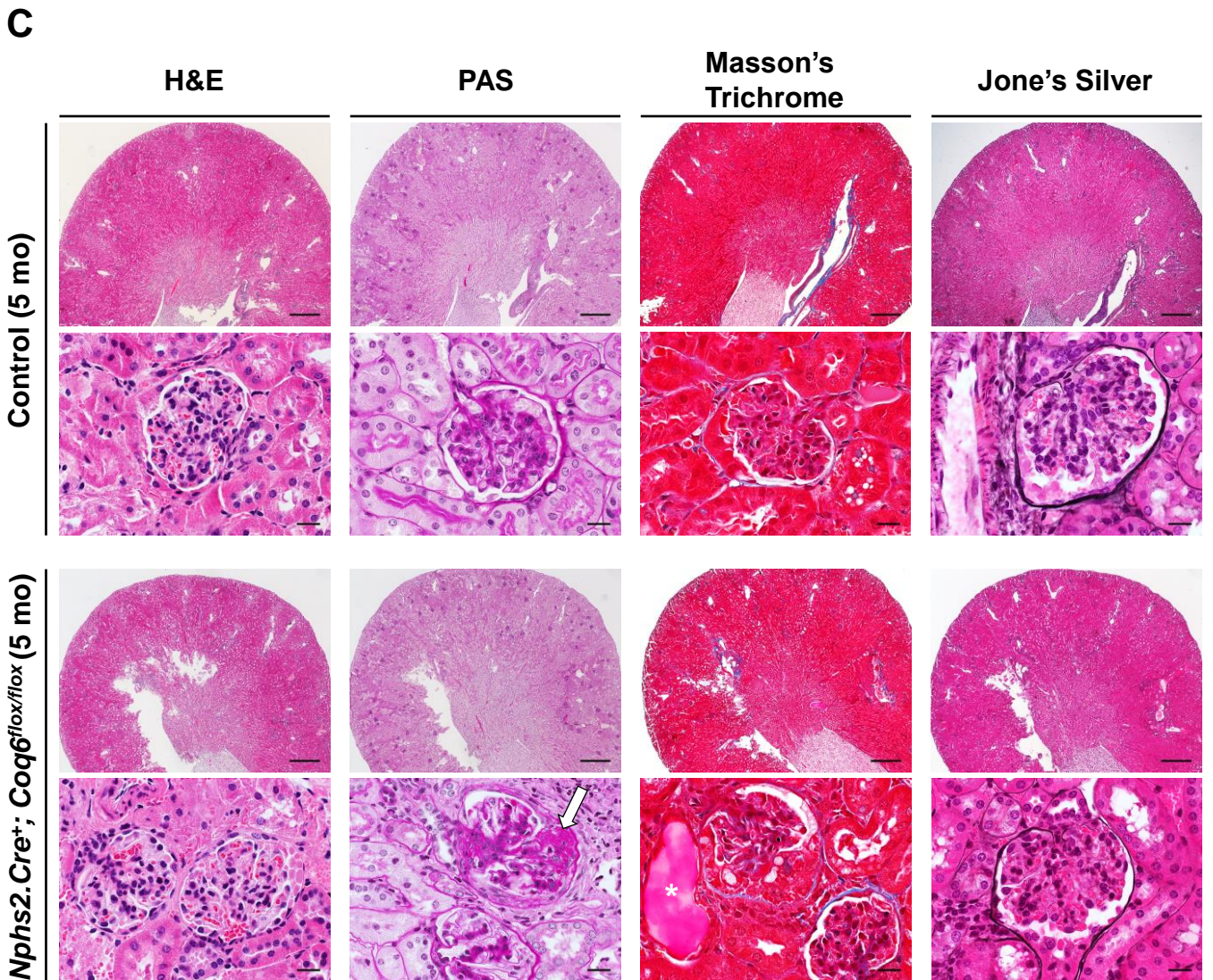
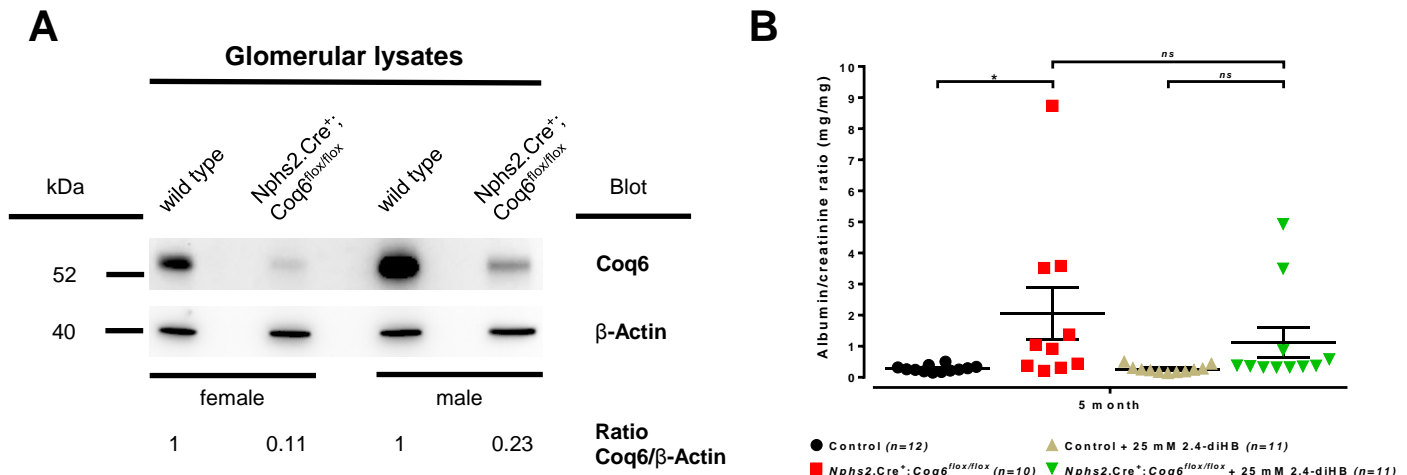
- **Supplementary Figure 1.** Generation and genotyping strategy for *Nphs2.Cre⁺;Coq6^{flox/flox}* mouse model.
- **Supplementary Figure 2.** At 5 month of age *Nphs2.Cre⁺;Coq6^{flox/flox}* mice exhibit proteinuria and renal histopathological changes consistent with focal segmental glomerular sclerosis.
- **Supplementary Figure 3.** *Coq6* knockout in *Nphs2.Cre⁺;Coq6^{flox/flox}* mutant mice leads to reduced physical condition and macroscopic morphological changes of kidneys.
- **Supplementary Figure 4.** *Coq6* knockout in *Nphs2.Cre⁺;Coq6^{flox/flox}* mutant mice causes focal segmental glomerular sclerosis. Treatment with 2.4-diHB prevents disease progression, resulting in normal histological findings.
- **Supplementary Figure 5.** Electron microscopy reveals podocyte foot process effacement in *Nphs2.Cre⁺;Coq6^{flox/flox}* mutant mice at 5 month of age.
- **Supplementary Figure 6.** Quantitative analysis of the expression of podocyte-specific proteins in *Nphs2.Cre⁺;Coq6^{flox/flox}* glomeruli.
- **Supplementary Figure 7.** *Nphs2.Cre⁺;Coq6^{flox/flox}* mice show increased glomerular fibrosis and staining for mesangial markers.
- **Supplementary Figure 8.** Quantitative analysis of the expression of the fibrotic markers α -SMA and Desmin in *Nphs2.Cre⁺;Coq6^{flox/flox}* glomeruli.
- **Supplementary Figure 9.** *Nphs2.Cre⁺;Coq6^{flox/flox}* mice develop renal fibrosis.
- **Supplementary Figure 10.** *Nphs2.Cre⁺;Coq6^{flox/flox}* mice show a reduced staining of podocytes specific markers.
- **Supplementary Figure 11.** Deletion of *Coq6* leads to morphological abnormalities in podocyte mitochondria.

- **Supplementary Figure 12.** COQ6 siRNA mediated transient knockdown reduce podocyte migration rate of cultured human podocytes with full rescue by 2,4-diHB, partial rescue by vanillic acid and absent rescue by 3,4-diHB.

A**B****C**

Supplementary Figure 1. Generation and genotyping strategy for $Nphs2.Cre^+;Coq6^{flox/flox}$ mouse model.

(A) Schematic diagram of reporter-tagged cassette insertion (2) in $Coq6$ wild type locus (1) including status post site-directed recombination using Flp-FRT technology (3) to generate $Coq6$ conditional knock-out locus following by use of Cre-LoxP technology (4) to generate tissue specific $Coq6$ knock-out. Genotyping primer locations are indicated with numbers 70,72,73,82 and 275. Exons are indicated with numbers. (B) Genotyping PCR products from tail tips. Primers 70/82 generate 352 bp product from wild type locus (black arrow) and 566 bp product from LoxP-containing conditional knockout locus (blue arrow) located upstream of Exon 6. Primers 72/73 generate 414 bp product from LoxP-containing conditional knockout locus (purple arrow) located downstream of Exon 6. Internal PCR control generate 210 bp product (green arrow) confirming DNA presence in each reaction except the water control. (C) Tissue specific genotyping PCRs of kidney, liver and heart. Primers 275/73 generate 1268 bp product in all tissues (purple arrow) showing mutant locus presence in each reaction except water control. The 447 bp product (black arrow) occurs only in $NPHS2.Cre^+;Coq6^{flox/floxP}$ animals indicating podocytes specific $NPHS2$; Cre mediated locus recombination.



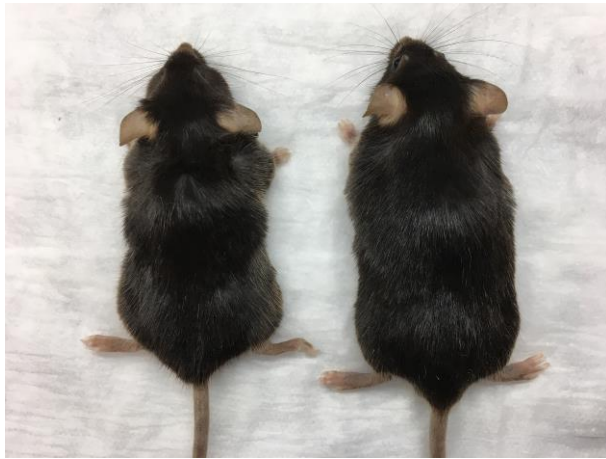
Supplementary Figure 2

Supplementary Figure 2. At 5 month of age *Nphs2.Cre⁺;Coq6^{flox/flox}* mice exhibit proteinuria and renal histopathological changes consistent with focal segmental glomerular sclerosis.

(A) Western blot analysis confirms significant reduction of Coq6 in glomerular lysates of the *Nphs2.Cre⁺;Coq6^{flox/flox}* mutant mice. Findings were confirmed in two independent experiments (technical western blot repeats), displayed blot shows representative image.

(B) Urinary albumin/creatinine ratio analysis reveals onset of proteinuria at age of 5 month in *Nphs2.Cre⁺;Coq6^{flox/flox}* mutant mice. Each data point represents technical duplicate. One-way ANOVA *p*-values calculated using Tukey's multiple comparisons test are shown in the figure (*ns*=not significant, * *p*<0.05, error bars represent mean +/- SEM).

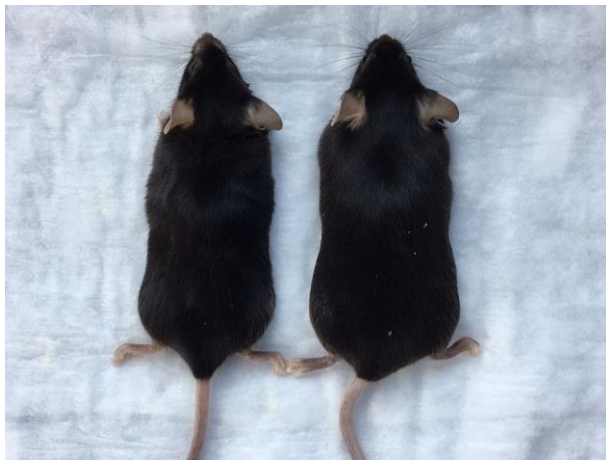
(C) Kidney serial sections and representative images of 5 month old animals at indicated genotypes were stained accordingly to indicated conditions. Note the presence of focal segmental glomerulosclerotic changes with synechia (white arrow) in *Nphs2.Cre⁺;Coq6^{flox/flox}* mutant mice. Asterisks mark proteinaceous casts in dilated tubules of the *Nphs2.Cre⁺;Coq6^{flox/flox}* mutant mice. (Scale bars: upper rows 500 μ m and lower rows 20 μ m).

A*NPHS2.Cre⁺;Coq6^{flox/flox}*

Control

B*NPHS2.Cre⁺;Coq6^{flox/flox}*

Control

C*NPHS2.Cre⁺;Coq6^{flox/floxP}*
+ 25 mM 2.4-diHBControl
+ 25 mM 2.4-diHB**D***NPHS2.Cre⁺;Coq6^{flox/flox}*
+ 25 mM 2.4-diHBControl
+ 25 mM 2.4-diHB

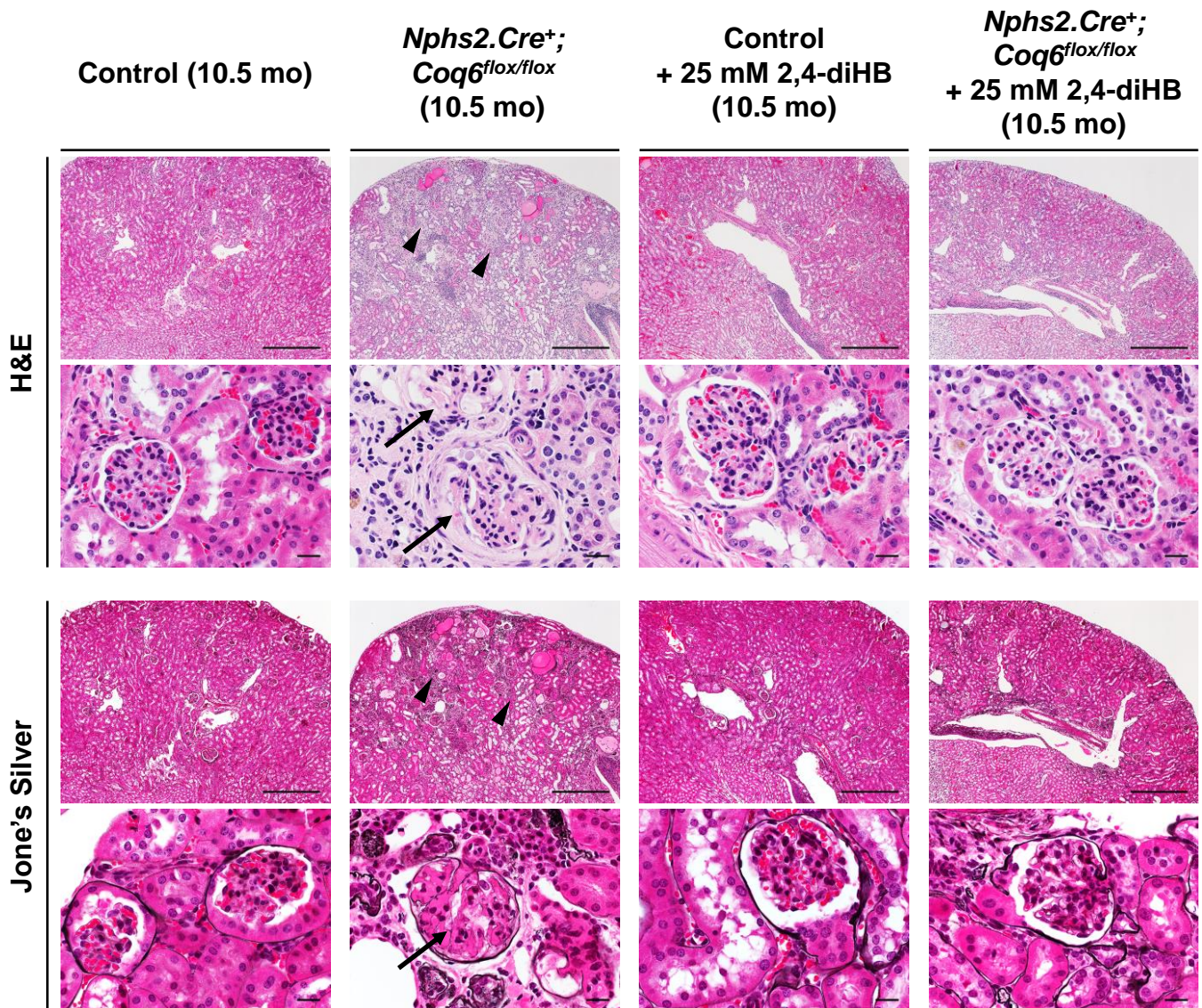
Supplementary Figure 3. *Coq6* knockout in *Nphs2.Cre⁺;Coq6^{flox/flox}* mutant mice leads to reduced physical condition and macroscopic morphological changes of kidneys.

(A) Representative image of 10.5 month old mice at indicated genotypes. *Nphs2.Cre⁺;Coq6^{flox/flox}* mutant mouse showed progressive reduction of physical condition compared to littermates controls.

(B) Representative image of kidneys from 10.5 month old mice at indicated genotypes. *Nphs2.Cre⁺;Coq6^{flox/flox}* mutant mouse showed macroscopic changes of kidneys compared to littermates controls.

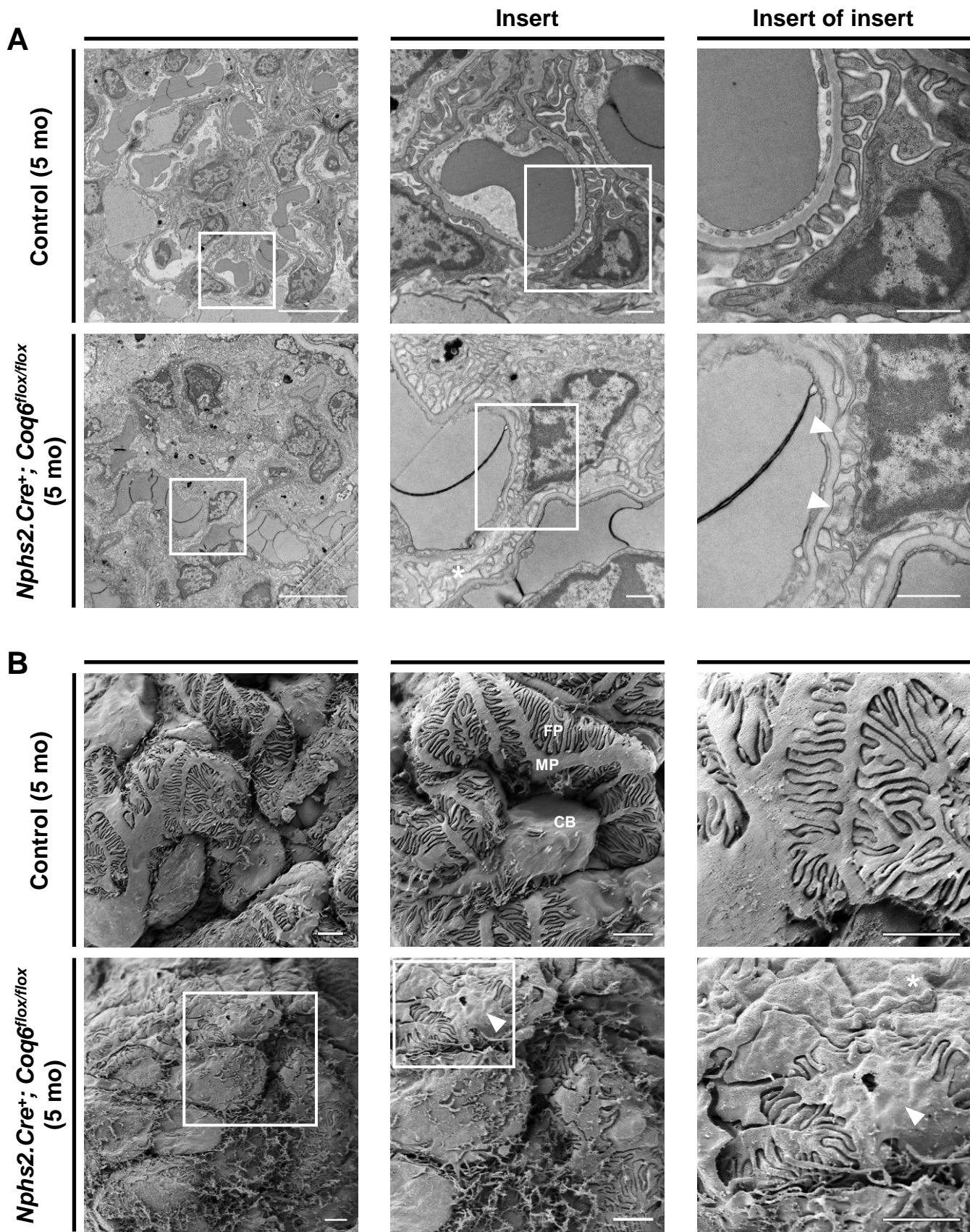
(C) Representative image of 10.5 month old mice at indicated genotypes. *Nphs2.Cre⁺;Coq6^{flox/flox}* mutant mouse treated with 25 mM 2.4-diHB showed normal physical condition compared to littermates controls.

(D) Representative image of kidneys from 10.5 month old mice at indicated genotypes. *Nphs2.Cre⁺;Coq6^{flox/flox}* mutant mouse treated with 25 mM 2.4-diHB showed normal macroscopic appearance of kidneys show macroscopic changes of kidneys compared to littermates controls under the same treatment.



Supplementary Figure 4. *Coq6* knockout in *Nphs2.Cre⁺;Coq6^{flox/flox}* mutant mice causes focal segmental glomerular sclerosis. Treatment with 2,4-diHB prevents disease progression, resulting in normal histological findings.**

Kidney serial sections and representative images of 10.5 month old mice at indicated genotypes were stained according to indicated conditions. The *Nphs2.Cre⁺;**Coq6^{flox/flox}* mutant mice showed focal segmental glomerular sclerosis (arrows) with focal interstitial fibrosis and tubular atrophy (arrow heads). In contrast, *Nphs2.Cre⁺;**Coq6^{flox/flox}* mutant mice under treatment with 2,4-diHB showed normal histological kidney morphology (Scale bars: upper rows 500 μ m and lower rows 20 μ m).

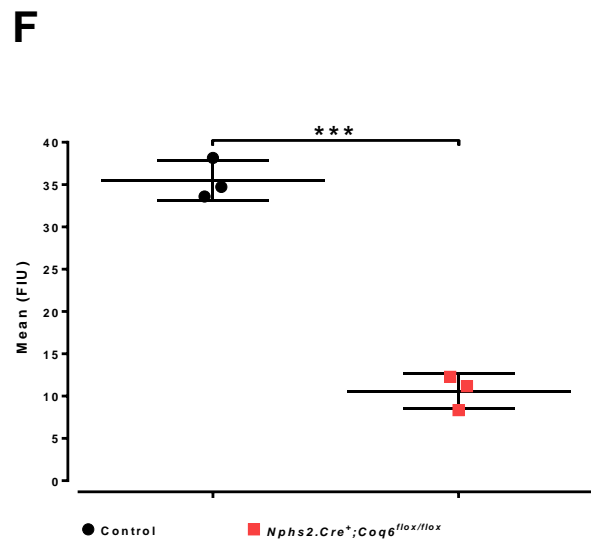
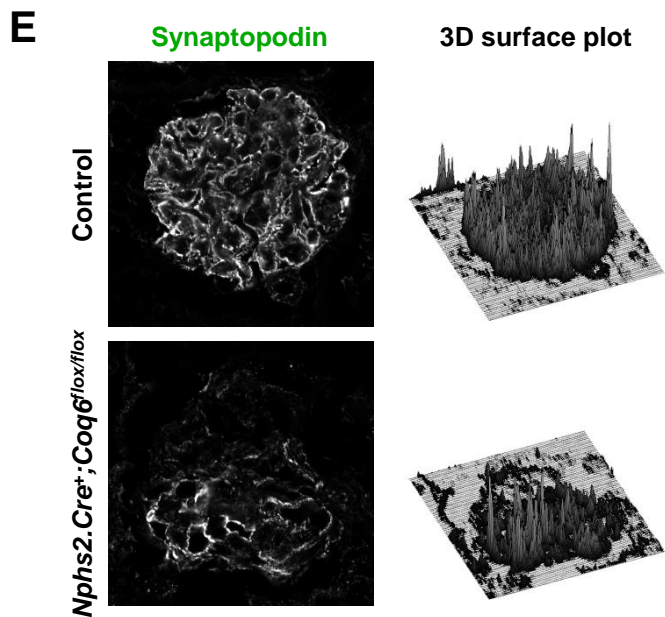
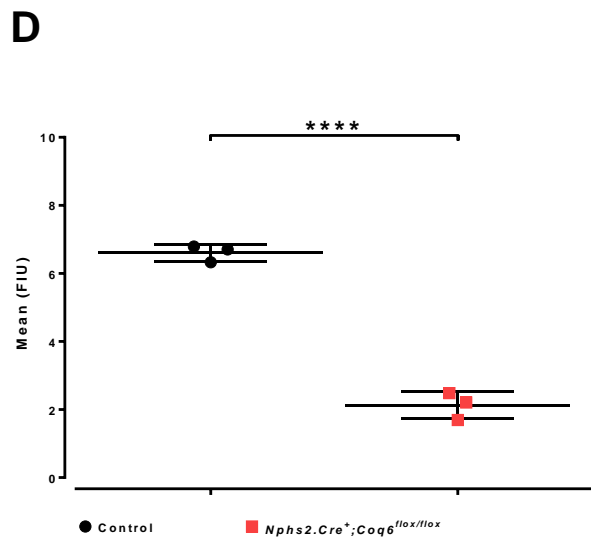
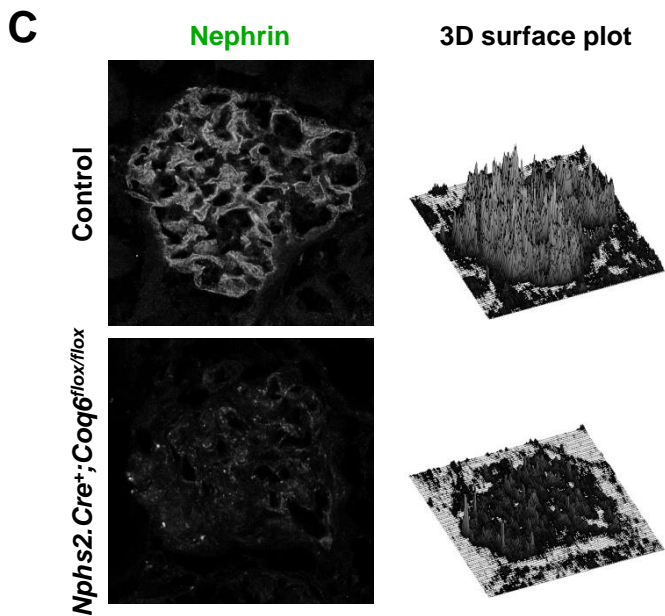
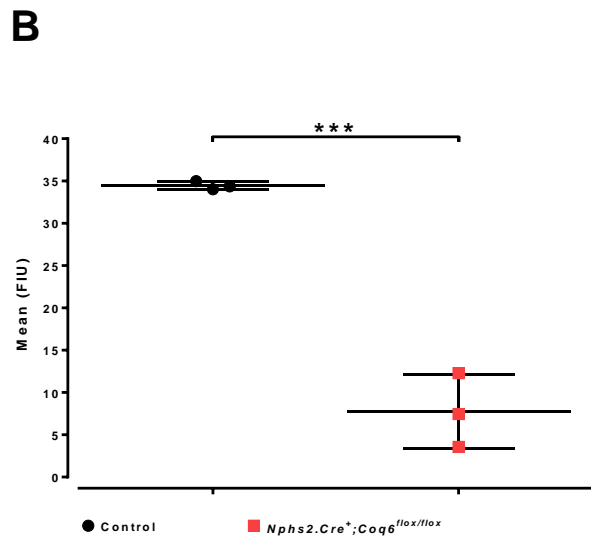
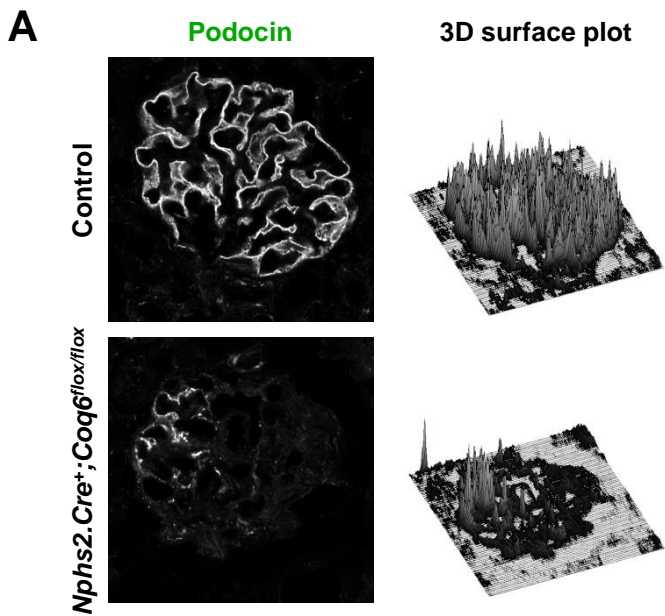


Supplementary Figure 5

Supplementary Figure 5. Electron microscopy reveals podocyte foot process effacement in *Nphs2.Cre⁺;Coq6^{flox/flox}* mutant mice at 5 month of age.

(A) Transmission electron microscopy representative images of 5 month old mice at indicated genotypes. Control mice showed normal glomerular ultrastructure, whereas glomerular ultrastructure of *Nphs2.Cre⁺;Coq6^{flox/flox}* mutant mice revealed coarsening (arrow heads) of foot processes. ($n=2$ mice in each group. Scale bars: 10 μm left panel, 1 μm middle panel, and 2 μm right panel).

(B) Scanning electron microscopy representative images of 5 month old mice at indicated genotypes. In control mice images showed normal major processes (MP) and foot processes (FP) of podocytes. In *Nphs2.Cre⁺;Coq6^{flox/flox}* mutant mice podocytes major processes appear enlarged (arrow heads) and foot processes of podocytes display regional effacement (asterisks). The cell bodies (CB) of podocytes in *Nphs2.Cre⁺;Coq6^{flox/flox}* mutant mice display microvilli like structures on their surface. ($n=2$ mice in each group. Scale bars in all panels 2 μm).

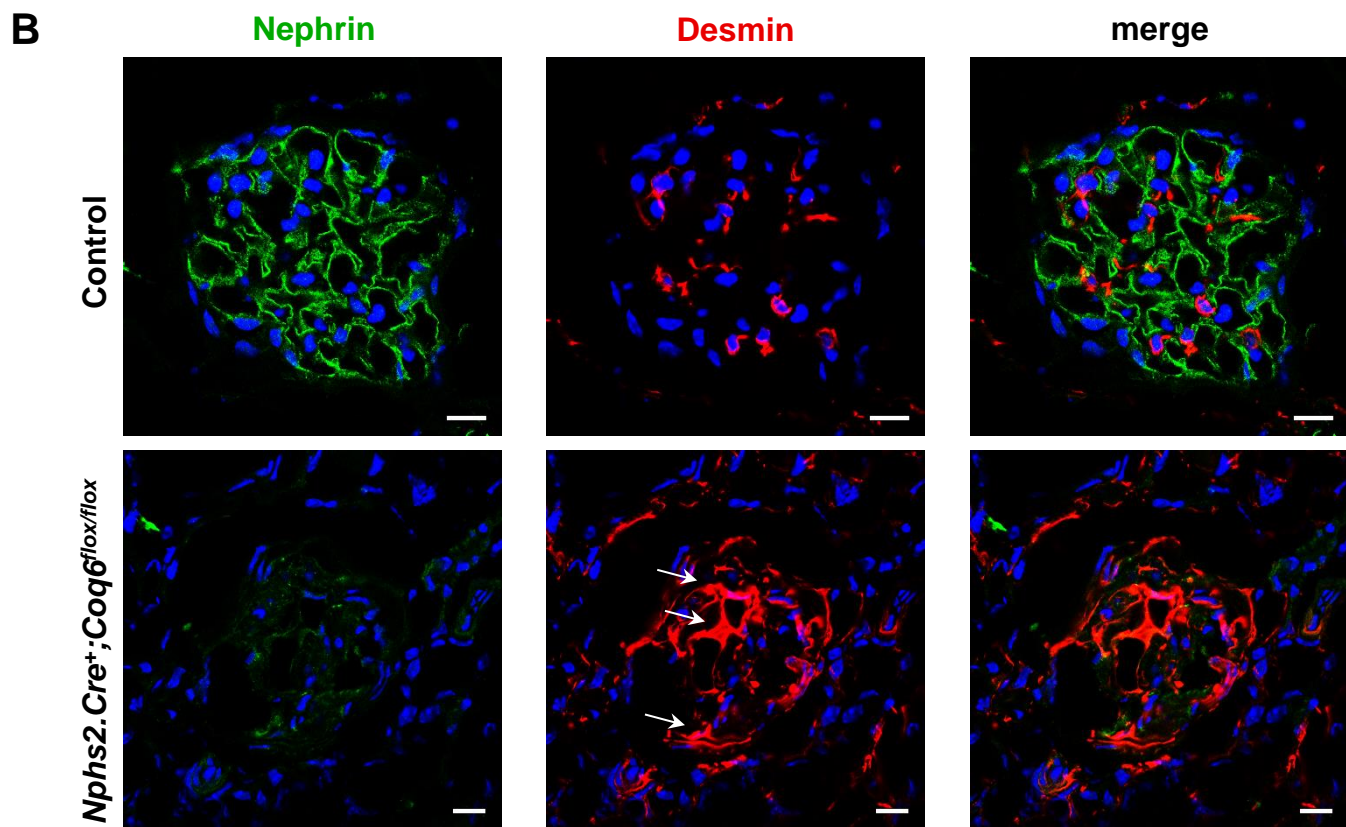
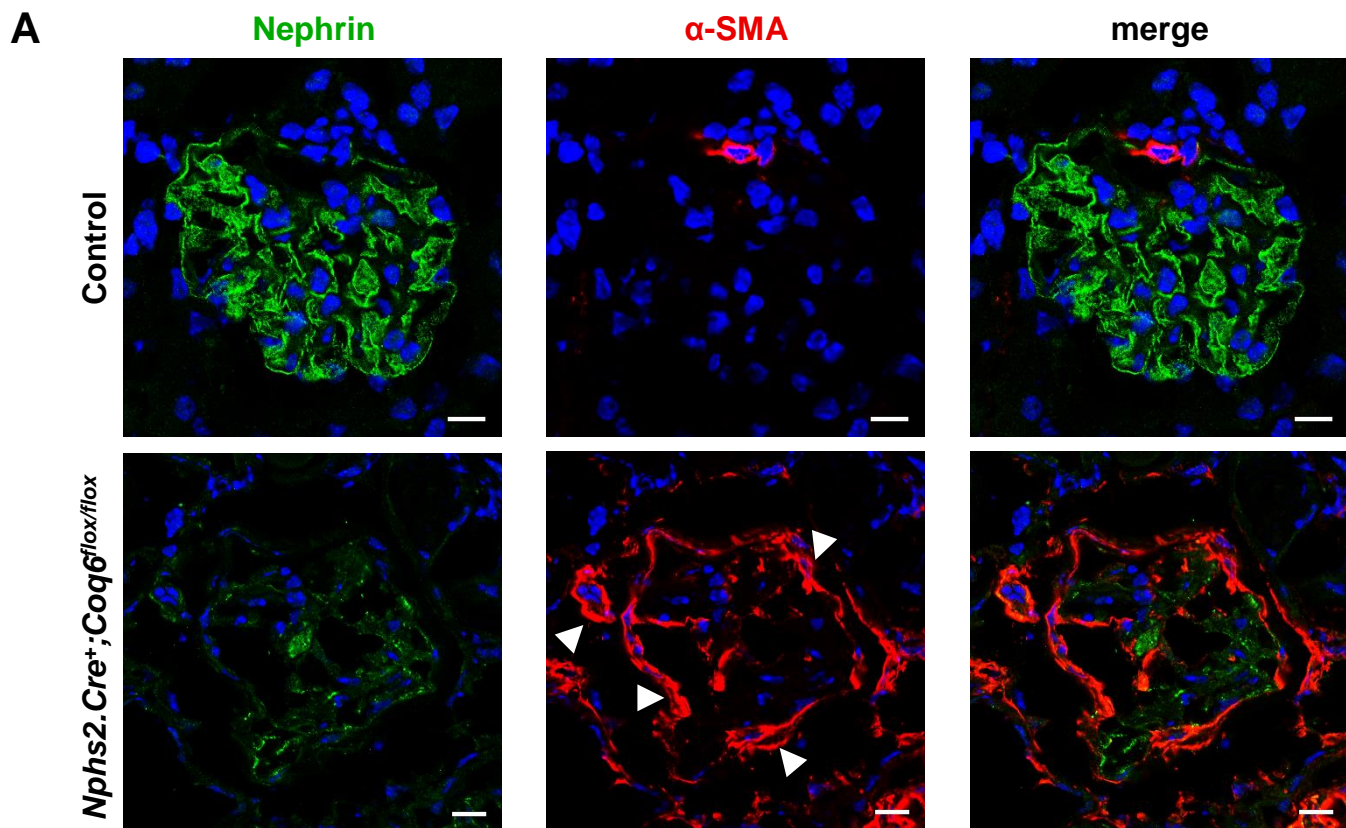


Supplementary Figure 6

Supplementary Figure 6. Quantitative analysis of the expression of podocyte-specific proteins in *Nphs2.Cre⁺;Coq6^{flox/flox}* glomeruli.

(A), (C) and (E) Immunofluorescence staining of frozen kidney sections from control and *Nphs2.Cre⁺;Coq6^{flox/flox}* 10.5 month old mice against the slit diaphragm proteins podocin (A) and nephrin (C), and podocyte foot-process marker synaptopodin (E). A 3D surface plot depicting the respective antibody staining intensities is shown on the right. Normal expression levels of podocin, nephrin and synaptopodin are seen in control mice. *Nphs2.Cre⁺;Coq6^{flox/flox}* mice show reduced podocin expression (A), globally reduced nephrin expression (C) and reduced synaptopodin expression (E).

(B), (D) and (F) Quantification of antibody staining in (A), (C) and (E) respectively, demonstrates a significantly decreased expression of podocin (B), nephrin (D) and synaptopodin (F) in *Nphs2.Cre⁺;Coq6^{flox/flox}* glomeruli compared to control glomeruli (FIU=fluorescence intensity units, $n=3$ images in each group were analysed, p -values were calculated using an unpaired t -test; *** $p<0.001$, **** $p<0.0001$, error bars represent SD).

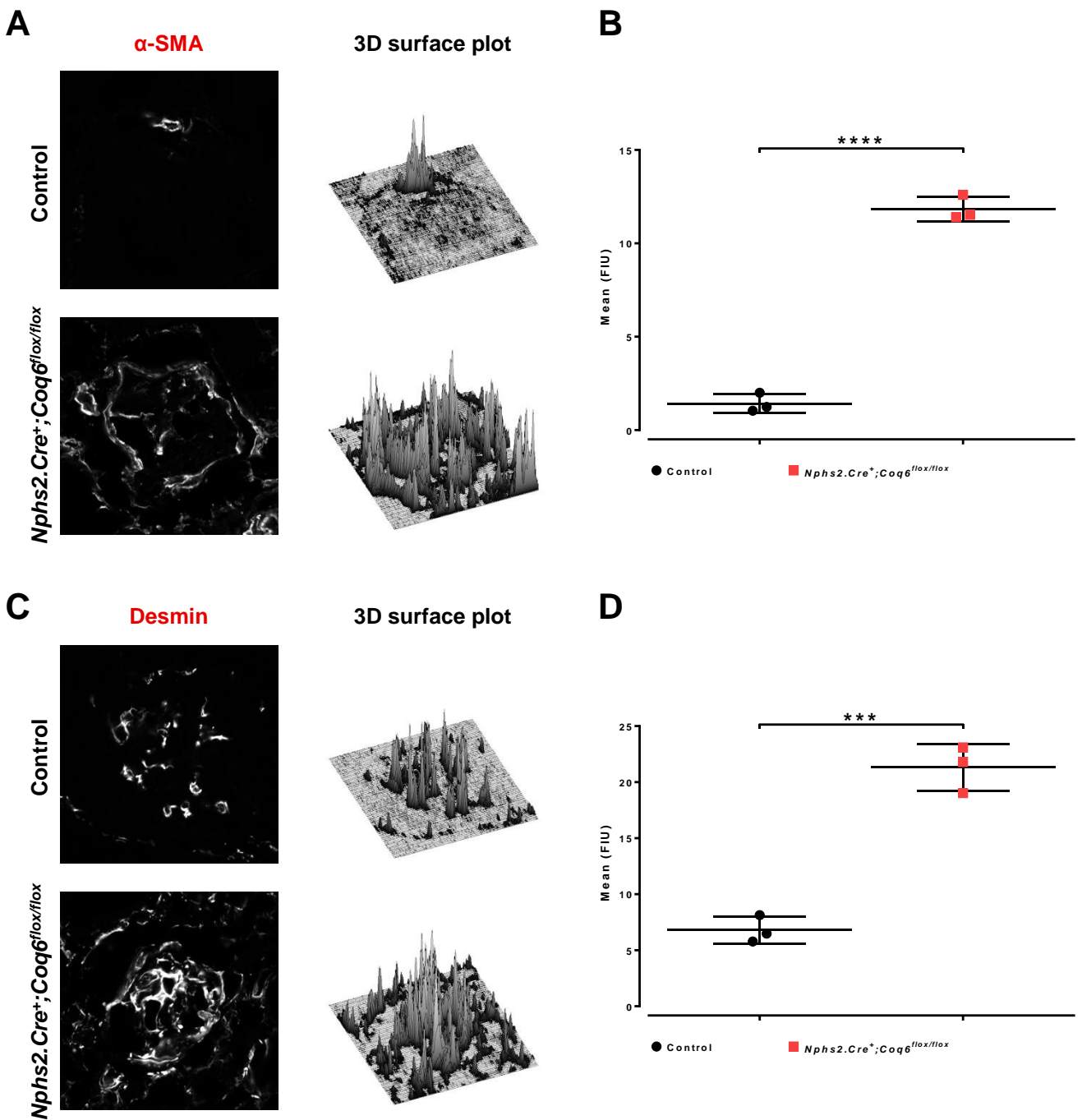


Supplementary Figure 7

Supplementary Figure 7. *Nphs2.Cre⁺;Coq6^{flox/flox}* mice show increased glomerular fibrosis and staining for mesangial markers.

(A) Staining of frozen kidney sections and representative images at 10.5 month old mice for the slit diaphragm protein nephrin as well as for the glomerular fibrosis marker smooth muscle actin (α -SMA). A normal expression pattern of nephrin and α -SMA is seen in control mice. In contrast, *Nphs2.Cre⁺;Coq6^{flox/flox}* mutant mice showed globally decreased nephrin staining, whereas α -SMA staining (arrow heads) is focally increased (Scale bars: 10 μ m).

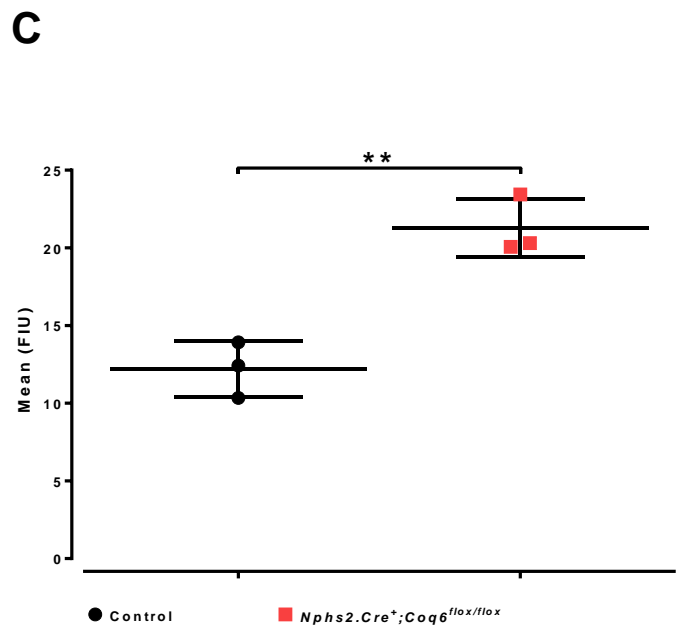
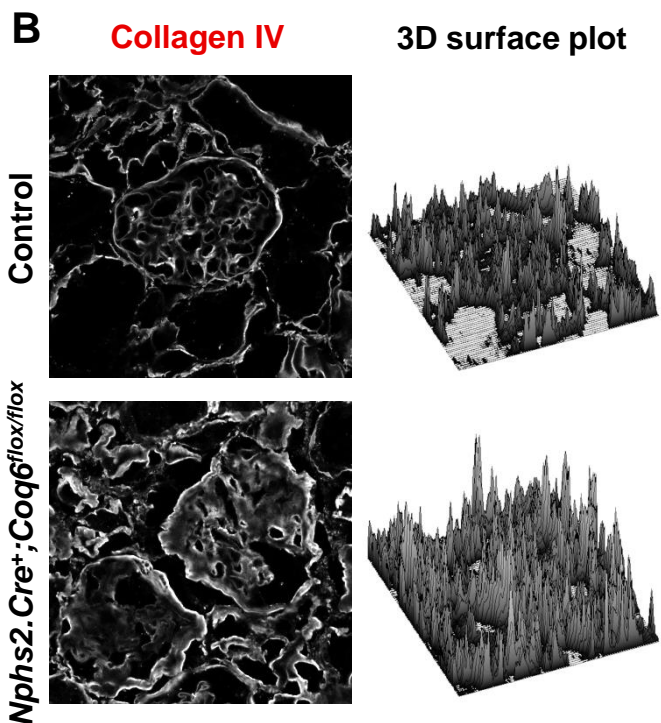
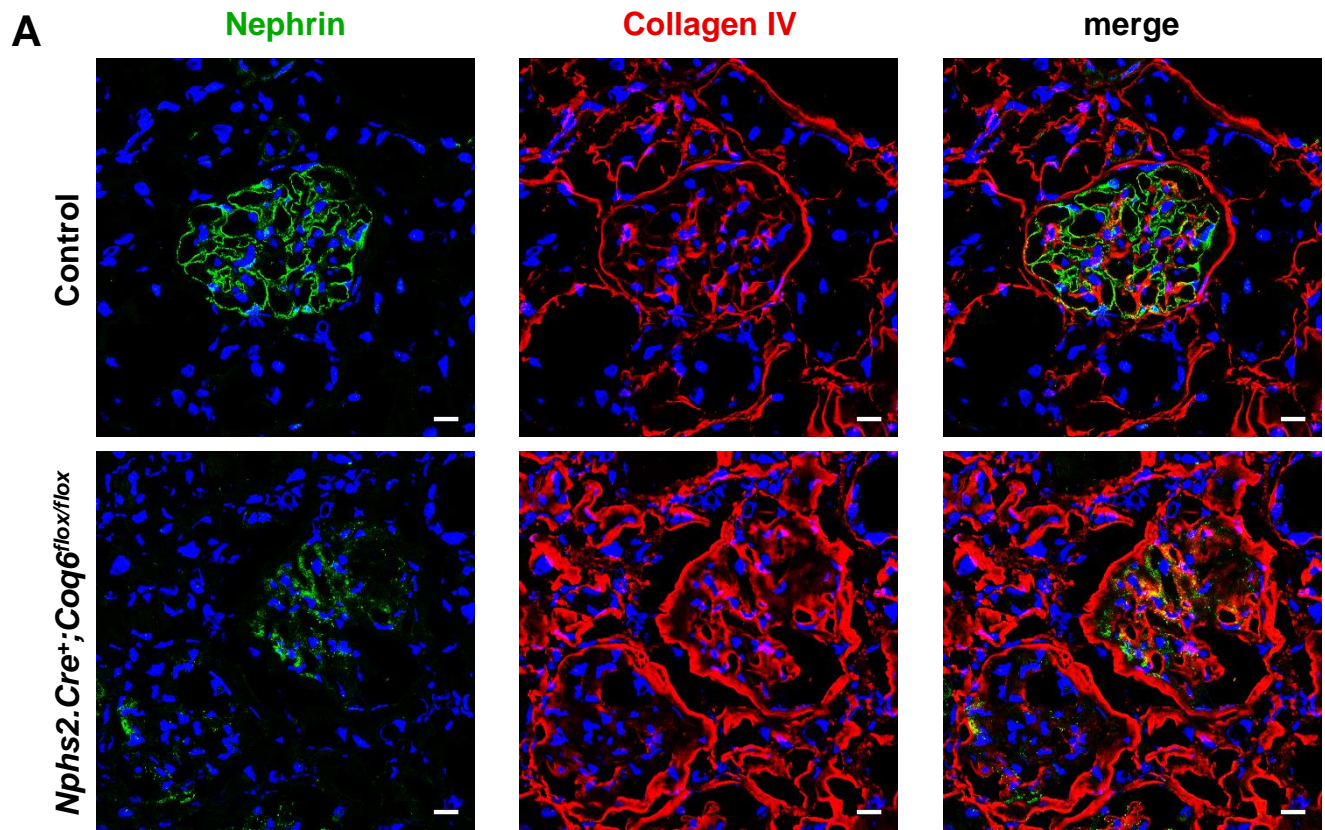
(B) Staining of frozen kidney sections and representative images at 10.5 month old mice for the slit diaphragm protein nephrin as well as for the mesangial marker desmin. A normal expression pattern of nephrin and desmin is seen in control mice. In contrast, *Nphs2.Cre⁺;Coq6^{flox/flox}* mutant mice showed reduced nephrin staining, whereas mesangial desmin expression (arrows) is increased (Scale bars: 10 μ m).



Supplementary Figure 8. Quantitative analysis of the expression of the fibrotic markers α-SMA and Desmin in *Nphs2.Cre⁺;Coq6^{flox/flox}* glomeruli.

(A) and (C) Immunofluorescence staining of frozen kidney sections from control and *Nphs2.Cre⁺;Coq6^{flox/flox}* 10.5 month old mice against the glomerular fibrosis markers smooth muscle actin (α-SMA) and desmin. A 3D surface plot depicting the respective antibody staining intensities shown on the right. α-SMA and desmin are expressed at low levels in control mice. In contrast, *Nphs2.Cre⁺;Coq6^{flox/flox}* mice have increased α-SMA and desmin expression levels.

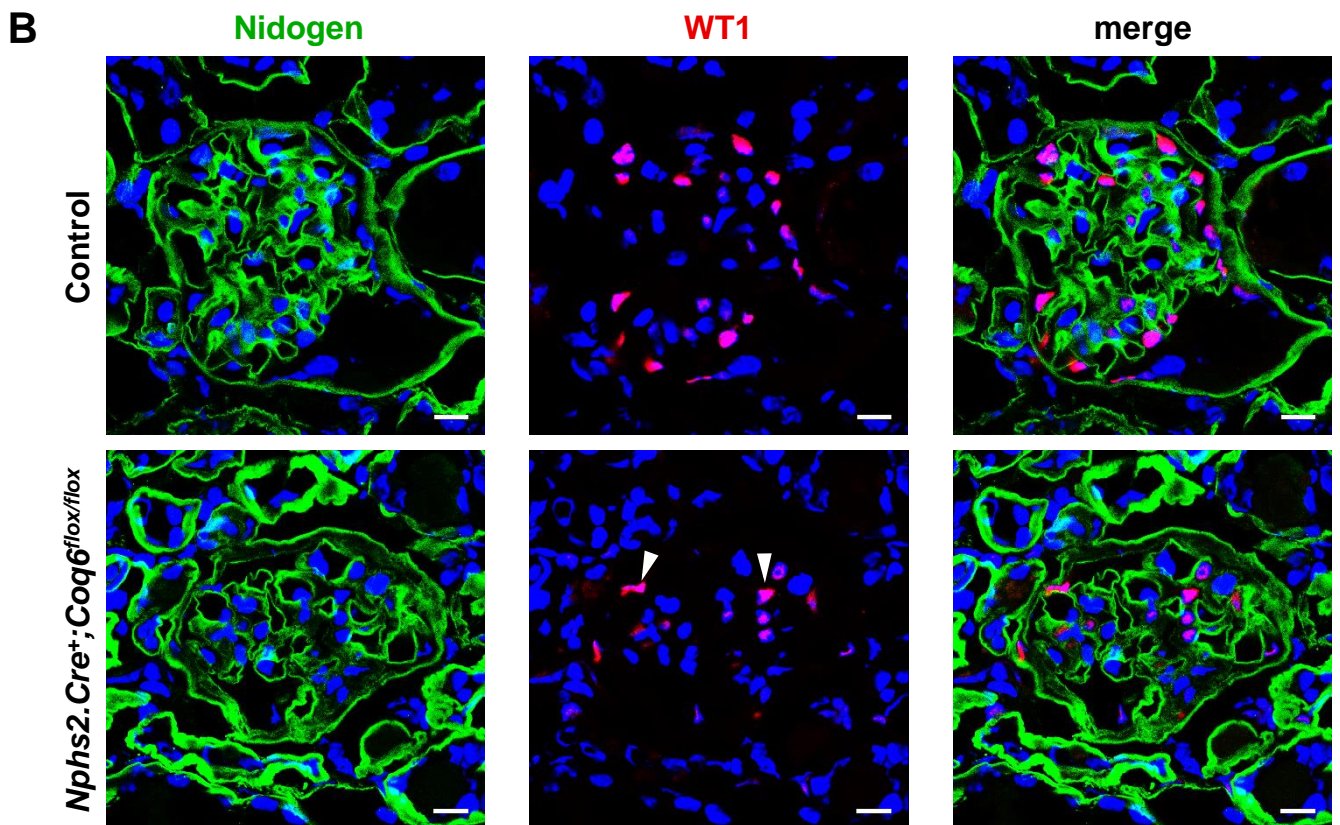
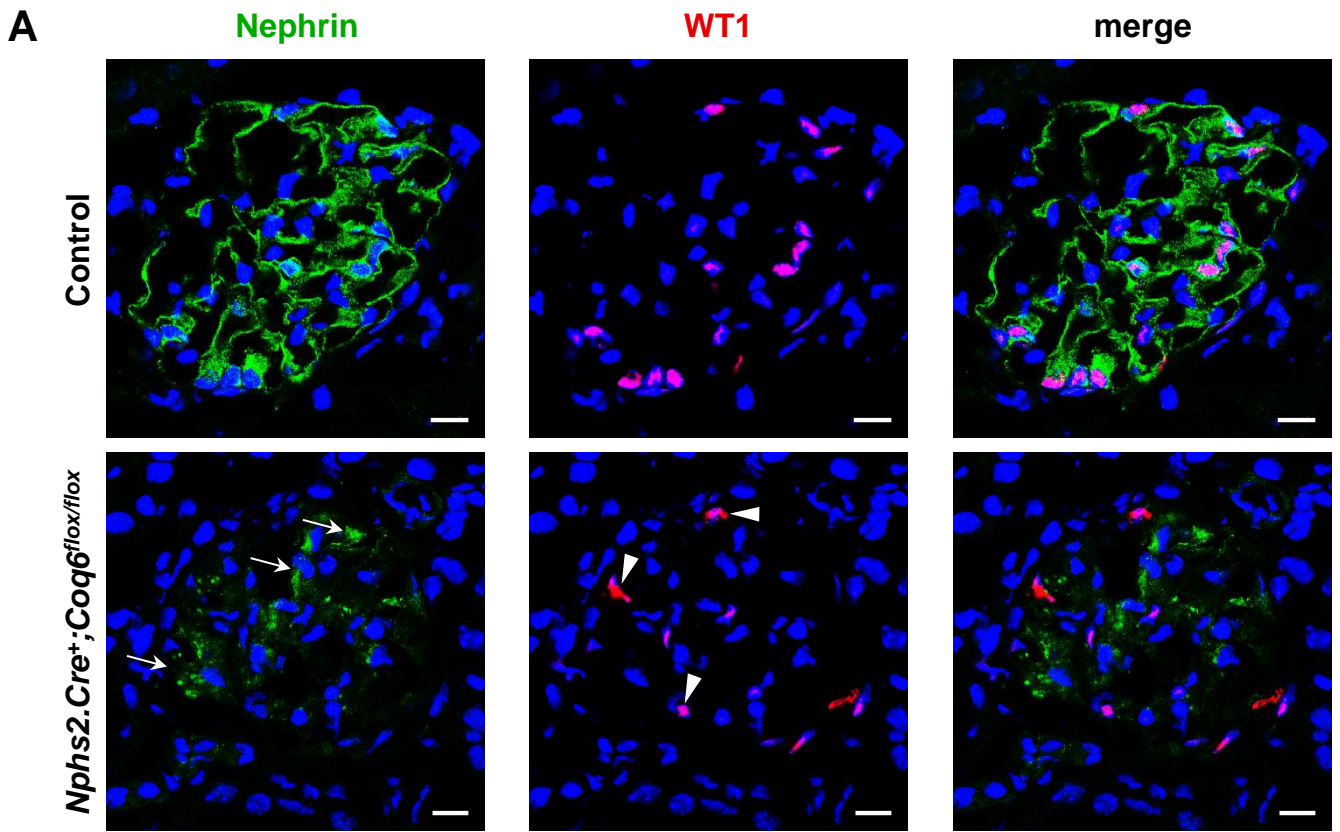
(B) and (D) Quantification of antibody staining in (A) and (C) respectively, demonstrates a significant increase in α-SMA and desmin expression in *Nphs2.Cre⁺;Coq6^{flox/flox}* glomeruli compared to control glomeruli (FIU=fluorescence intensity units, $n=3$ images in each group were analysed, p -values were calculated using an unpaired t -test; *** $p<0.001$, **** $p<0.0001$, error bars represent SD).



Supplementary Figure 9. *Nphs2.Cre⁺;Coq6^{flox/flox}* mice develop renal fibrosis.

(A) and (B) immunofluorescence staining of frozen kidney sections from control and *Nphs2.Cre⁺;Coq6^{flox/flox}* 10.5 month old mice against slit diaphragm protein nephrin and fibrosis marker collagen IV. A 3D surface plot depicting the respective antibody staining intensities shown on the right (B). Normal expression levels of nephrin and collagen IV are seen in control glomeruli. In contrast, *Nphs2.Cre⁺;Coq6^{flox/flox}* glomeruli showed decreased nephrin expression, while collagen IV expression was increased, indicating fibrotic changes (Scale bars: 10 μ m).

(C) Quantification of antibody staining in (B), demonstrates a significantly increased expression of collagen IV in *Nphs2.Cre⁺;Coq6^{flox/flox}* mutant kidneys compared to control kidneys (FIU=fluorescence intensity units, $n=3$ images in each group were analysed, p -values were calculated using an unpaired t -test; ** $p < 0.01$, error bars represent SD).



Supplementary Figure 10.

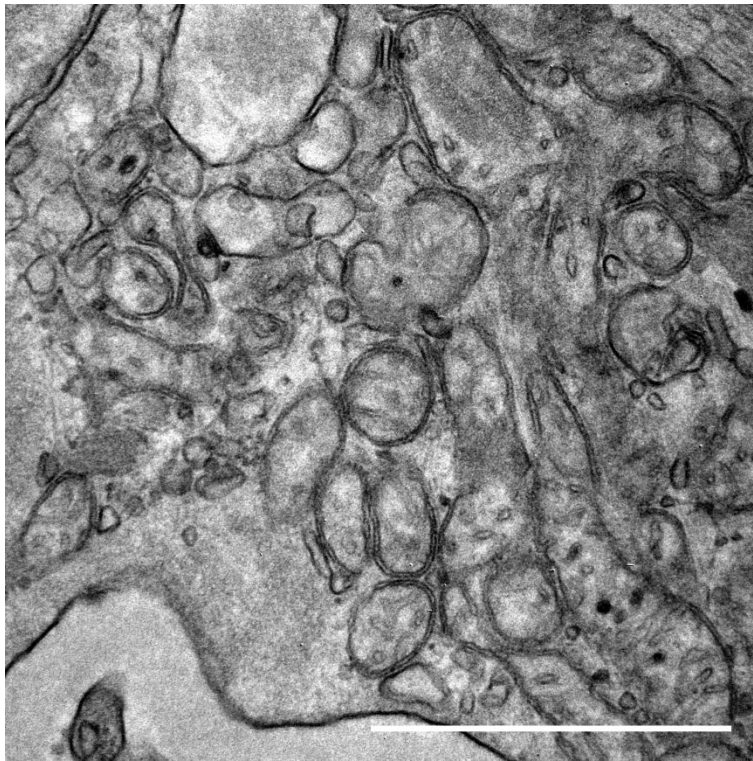
Supplementary Figure 10. *Nphs2.Cre⁺;Coq6^{flox/flox}* mice show a reduced staining of podocytes specific markers.

(A) Staining of frozen kidney sections and representative images at 10.5 month old mice for the slit diaphragm protein nephrin as well as for podocyte marker WT1 (Wilms tumor 1). A normal expression pattern of nephrin and WT1 is seen in control mice. In contrast, *Nphs2.Cre⁺;Coq6^{flox/flox}* mutant mice showed decreased staining of nephrin (arrows) and WT1 (arrow heads) (Scale bars: 10 μ m).

(B) Staining of frozen kidney sections and representative images at 10.5 month old mice for the basement membrane protein nidogen as well as for the podocytic marker WT1. A normal expression pattern of WT1 is seen in control mice. In contrast, *Nphs2.Cre⁺;Coq6^{flox/flox}* mutant mice showed decreased staining of WT1 (arrow heads) potentially indicating a reduced number of podocytes (Scale bars: 10 μ m).

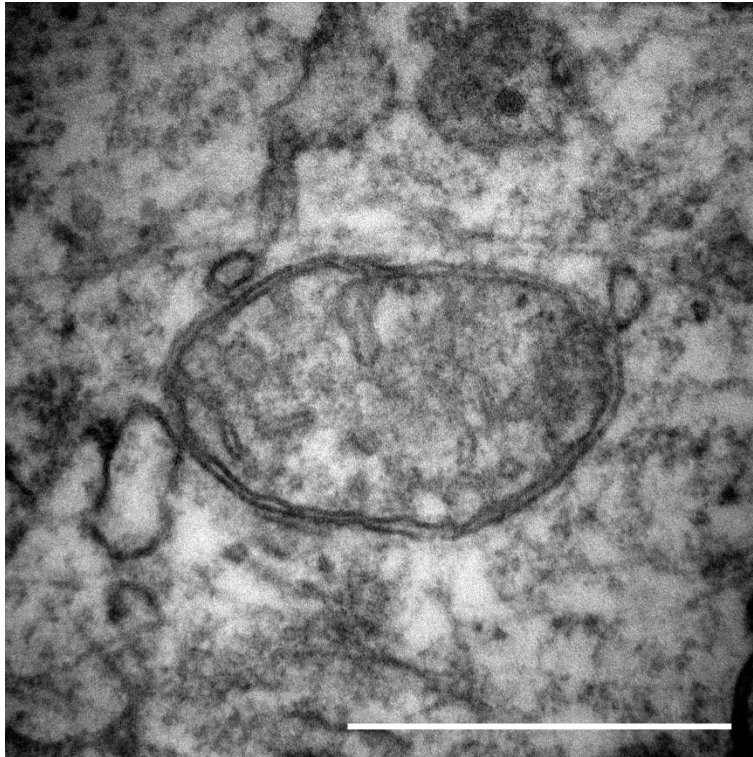
A

Nphs2.Cre⁺;Coq6^{flox/flox} (10.5 mo)



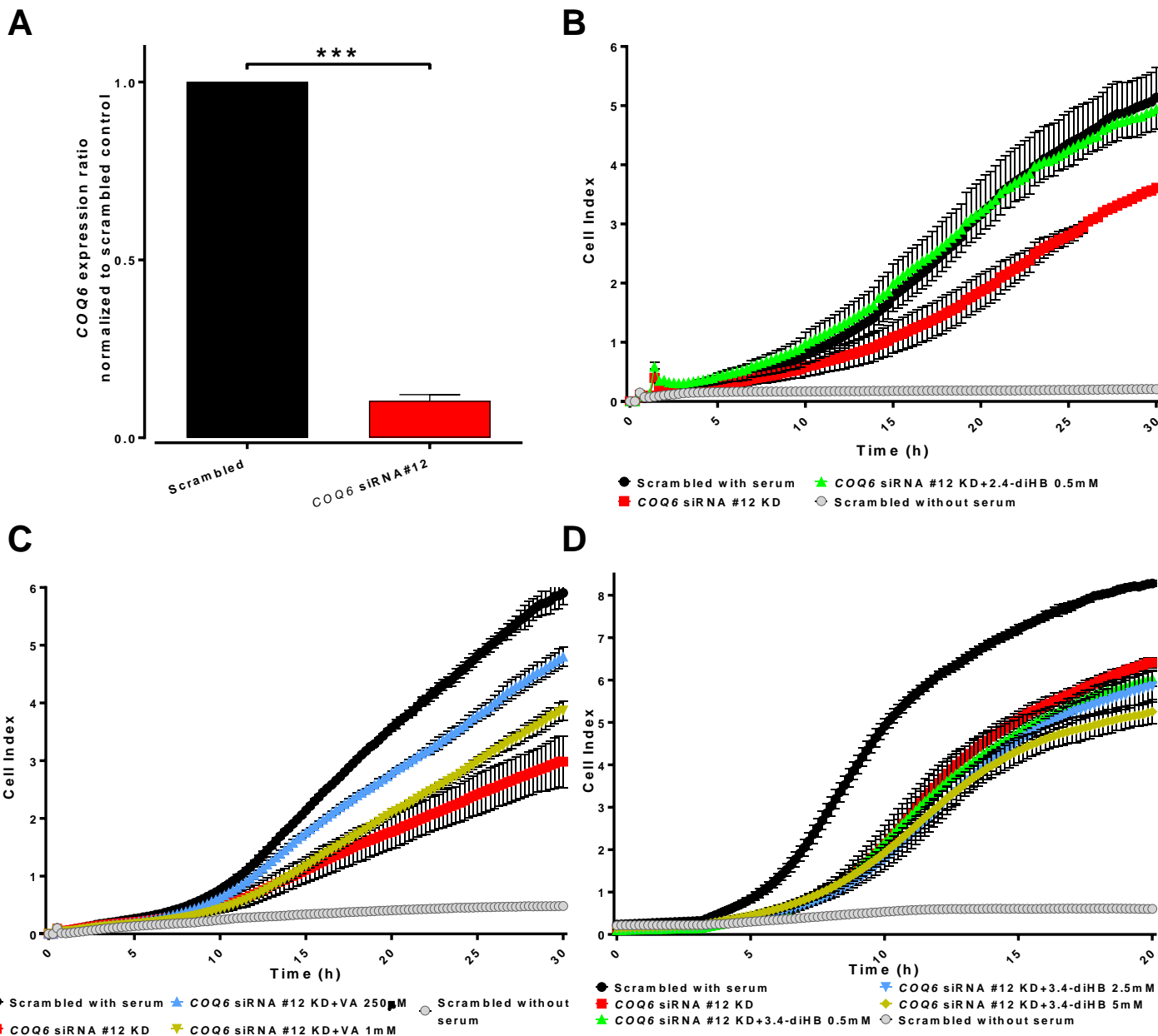
B

Nphs2.Cre⁺;Coq6^{flox/flox} (10.5 mo)



Supplementary Figure 11. Deletion of *Coq6* leads to morphological abnormalities in podocyte mitochondria.

(A) and **(B)** Transmission electron micrographs of 10.5 month old *Nphs2.Cre⁺;Coq6^{flox/flox}* podocyte mitochondria at high magnification. Mitochondria in *Nphs2.Cre⁺;Coq6^{flox/flox}* podocytes show abnormal morphology and perturbed mitochondrial matrix. Scale bars: (A) 1 μ m and (B) 500 nm.



Supplementary Figure 12. COQ6 siRNA mediated transient knockdown reduce podocyte migration rate of cultured human podocytes with full rescue by 2,4-diHB, partial rescue by vanillic acid and absent rescue by 3,4-diHB.

(A) Effect of COQ6 knockdown on mRNA level in human podocytes assed with qPCR technic using siRNA. The figure shows a representative experiment. Data points represent fold change of three technical replicates. The experiment was repeated in two independent cell culture experiments and normalized to scrambled control siRNA. Podocytes transfected with COQ6 siRNA show significant reduction of mRNA level for siRNA #12 compared to podocytes transfected with scrambled control siRNA (p -values were calculated using an unpaired t -test; *** $p < 0.001$, error bars represent SD).

(B) Podocytes transfected with COQ6 siRNA exhibited decreased serum-induced migration rate (red line) compared to podocytes transfected with scrambled control siRNA (black line). Decreased podocyte migration rate seen upon COQ6 siRNA knockdown was fully rescued by 2.4-diHB at indicated concentration (green line).

(C) Decreased podocyte migration rate seen upon COQ6 siRNA knockdown (red line) was partially rescued with vanillic acid at indicated concentrations (blue and yellow lines).

(D) Decreased podocyte migration rate seen upon COQ6 siRNA knockdown was not rescuable by 3.4-diHB at indicated concentrations (green, blue and yellow lines). The effect of COQ6 knockdown on cell migration rate of human podocytes was assed with xCELLigence system (B-D). The figure show representative experiments, data points represent mean value of three technical replicates, error bars display standard deviation, experiments were repeated in two independent cell culture experiments each in (B-D).